JOURNAL OF VIROLOGY, July 2005, p. 8090–8100 Vol. 79, No. 13
0022-538X/05/$08.00+0 doi:10.1128/JVI.79.13.8090–8100.2005

Extensive Syncytium Formation Mediated by the Reovirus FAST Proteins Triggers Apoptosis-Induced Membrane Instability

Jayme Salsman, Deniz Top, Julie Boutilier,† and Roy Duncan*

Department of Microbiology and Immunology, Dalhousie University, Halifax, Nova Scotia B3H 4H7, Canada

Received 12 December 2004/Accepted 23 February 2005

The fusion-associated small transmembrane (FAST) proteins of the fusogenic reoviruses are the only known examples of membrane fusion proteins encoded by nonenveloped viruses. While the involvement of the FAST proteins in mediating extensive syncytium formation in virus-infected and -transfected cells is well established, the nature of the fusion reaction and the role of cell-cell fusion in the virus replication cycle remain unclear. To address these issues, we analyzed the syncytial phenotype induced by four different FAST proteins: the avian and Nelson Bay reovirus p10, reptilian reovirus p14, and baboon reovirus p15 FAST proteins. Results indicate that FAST protein-mediated cell-cell fusion is a relatively nonleaky process, as demonstrated by the absence of significant [^{3}H]uridine release from cells undergoing fusion and by the resistance of these cells to treatment with hygromycin B, a membrane-impermeable translation inhibitor. However, diminished membrane integrity occurred subsequent to extensive syncytium formation and was associated with DNA fragmentation and chromatin condensation, indicating that extensive cell-cell fusion activates apoptotic signaling cascades. Inhibiting effector caspase activation or ablating the extent of syncytium formation, either by partial deletion of the avian reovirus p10 ectodomain or by antibody inhibition of p14-mediated cell-cell fusion, all resulted in reduced membrane permeability changes. These observations suggest that the FAST proteins do not possess intrinsic membrane-lytic activity. Rather, extensive FAST protein-induced syncytium formation triggers an apoptotic response that contributes to altered membrane integrity. We propose that the FAST proteins have evolved to serve a dual role in the replication cycle of these fusogenic nonenveloped viruses, with nonleaky cell-cell fusion initially promoting localized cell-cell transmission of the infection followed by enhanced progeny virus release from apoptotic syncytia and systemic dissemination of the infection.

The reovirus fusion-associated small transmembrane (FAST) protein family is comprised of an atypical group of membrane fusion proteins encoded by nonenveloped viruses. Different FAST proteins have been isolated from four of the five recognized species in the genus *Orthoreovirus*, family *Reoviridae* (16). These fusogenic reoviruses and their corresponding FAST proteins include the p10 homologues encoded by avian reovirus (ARV) and Nelson Bay reovirus (NBV), p15 from baboon reovirus (BRV), and p14 from reptilian reovirus (RRV) (12, 14, 53). Unlike the membrane fusion proteins encoded by enveloped viruses, the reovirus FAST proteins are nonstructural viral proteins and therefore are not involved in virus entry (14, 15, 53). Rather, these proteins are expressed in virus-infected cells and trafficked through the endoplasmic reticulum-Golgi pathway to the plasma membrane (52). Accumulation of the FAST proteins at the cell surface leads to fusion of virus-infected cells with neighboring uninfected cells, in both cell culture and virus-infected animals (12, 28, 36, 37). While the involvement of these unusual nonenveloped virus fusion proteins in cell-cell fusion and syncytium formation is well established (4, 13, 14, 54), relatively little is known about the nature of the fusion reaction or the role of the FAST proteins in the replication cycle of the fusogenic reoviruses.

The p10 proteins of ARV and NBV share 33% sequence identity and the same repertoire and arrangement of structural motifs (53). In contrast, the BRV p15 and RRV p14 FAST proteins possess no significant amino acid sequence identity to each other or to the p10 proteins, and each contains its own signature arrangement of structural motifs (Fig. 1) (12, 14). The shared biophysical properties that currently define the FAST protein family include (i) their small size (95 to 140 amino acids), (ii) a transmembrane domain that serves as a signal-anchor sequence (24) to direct a bitopic type III (N_{exo}/C_{cyt}) topology in the plasma membrane, (iii) modification by acylation (myristoylation or palmitoylation), (iv) an essential membrane-proximal polybasic region, and (v) a hydrophobic

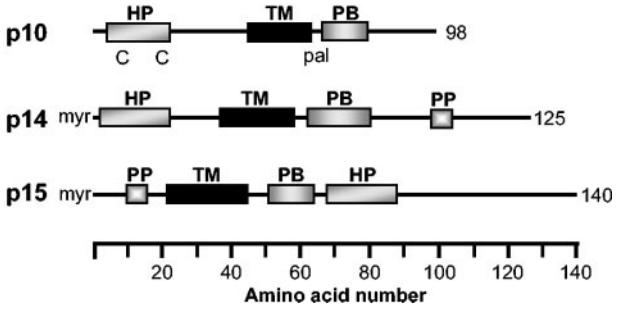

FIG. 1. FAST protein structural motifs. The linear arrangement of structural motifs present in the p10 (ARV or NBV), BRV p15, and RRV p14 reovirus FAST proteins is depicted. HP, hydrophobic patch; TM, transmembrane domain; PB, polybasic region; myr, myristoylation; pal, palmitoylation; PP, polyproline; C, cysteine residue.

* Corresponding author. Mailing address: Department of Microbiology and Immunology, Faculty of Medicine, Dalhousie University, Halifax, Nova Scotia B3H 4H7, Canada. Phone: (902) 494-6770. Fax: (902) 494-5125. E-mail: roy.duncan@dal.ca.

† Present address: Viral Diseases Division, Canadian Science Center for Human and Animal Health, 1015 Arlington Street, Winnipeg, Manitoba R3E 3R2, Canada.

patch, a second region of moderate hydrophobicity in addition to the transmembrane domain. Previous studies (4, 53) noted the similarity between the FAST proteins and a diverse group of viral membrane-interactive proteins, collectively referred to as viroporins (8). Viroporins are small (60 to 120 amino acids), often nonstructural, membrane-disruptive proteins with one or more hydrophobic motifs, frequently with an adjacent polybasic region. The membrane-destabilizing activity of viroporins may contribute to virus-induced cytopathic effects and to facilitating the release of both enveloped and nonenveloped viruses (6, 26, 41, 60).

Similar to the situation with viroporins, previous studies implicated the FAST proteins in reovirus egress. When ARV p10 trafficking to the plasma membrane is prevented, syncytium formation is inhibited, concurrent with delayed cell lysis and virus release (15). More recently, expression of ARV p10 in transfected cells was shown to alter membrane permeability (4), leading to the proposal that p10 functions as a membrane-destabilizing viroporin. The BRV p15 and RRV p14 proteins were only recently discovered (12, 14), and there are no data to indicate whether these FAST proteins share the membranelytic properties ascribed to the ARV p10 protein. The proposed membrane-lytic properties of p10 provide a possible explanation for the correlation between the extent of ARV-induced syncytium formation and viral pathogenesis (17), suggesting that the FAST proteins may function to promote cell lysis and virus release, thereby contributing to the natural pathogenicity of the fusogenic reoviruses (40, 59, 61).

It has been suggested that the membrane-destabilizing and membrane fusion activities of the ARV p10 protein represent distinct phenomena mediated by different protein domains (4). This conclusion was based on the observation that a fusion-negative (fusion-minus) construct of p10 retained the ability to alter plasma membrane integrity, leading to the proposal that enhanced virus release from ARV-infected cells reflects the membrane-destabilizing viroporin-like activity of the p10 FAST protein. As a result, it is unclear whether FAST protein-induced syncytium formation is a mere consequence of a viroporin-like membrane-destabilizing activity or whether membrane fusion proceeds through a series of specific lipid rearrangements similar to what is envisioned during membrane fusion mediated by enveloped virus fusion proteins (33). In other words, are the FAST proteins viroporins that happen to induce cell-cell fusion, or are they membrane fusion proteins that happen to induce altered membrane integrity? The p10 viroporin data also raise the question of what, if any, role is served by cell-cell fusion during the replication cycle of these nonenveloped viruses.

To begin to address the interrelationship between FAST protein-induced syncytium formation, altered membrane integrity, and the virus replication cycle, we analyzed the syncytium-inducing and membrane-lytic properties of both the ARV and NBV p10 proteins as well as the more recently discovered BRV p15 and RRV p14 proteins. For all members of the FAST protein family, membrane permeabilization was completely dependent on prior extensive syncytium formation. Furthermore, inhibiting effector caspase activation had no effect on syncytium formation but reduced membrane lysis. Based on these results, we propose that the FAST proteins function as specific membrane fusion proteins, serving a dual role in the virus replication cycle, mediating nonleaky membrane fusion and early cell-cell transmission of the infection followed by apoptosis-mediated disruption of syncytia and dissemination of the infection.

MATERIALS AND METHODS

Cells, virus, and reagents. Vero and QM5 cells were maintained in Earle's medium 199 as previously described (12). The production of p14 polyclonal antiserum was previously described (12). Avian reovirus strain SK138a (ARV-138) has been previously described (17). The creation of cDNA clones of the four FAST proteins and the ARV p10 deletion construct, all in the pcDNA3 mammalian expression vector, were previously described (12, 14, 53).

Infection, transfection, and syncytial indexing. Twelve-well cluster plates of QM5 cells at approximately 70% confluence were either infected (multiplicity of infection [MOI] = 5) or transfected using 1 μg of plasmid DNA and Lipofectamine (Invitrogen) as per the manufacturer's instructions. At 5 h posttransfection, the transfection mix was removed, cells were washed with phosphate-buffered saline (PBS), and fresh growth medium was added. At the indicated times postinfection/posttransfection, cells were fixed and stained with Wright-Giemsa stain as previously described (12). In some experiments, cells were treated with 50 μM of the general caspase inhibitor Z-VAD-fmk (Calbiochem) to prevent caspase cleavage and propagation of potential apoptotic signaling. Stained monolayers were examined by light microscopy, and a syncytial index (SI) was qualitatively scored on a scale of 0 to 4 based on the extent of syncytium formation: when SI was 0, monolayers were devoid of fusion; when SI was 1, there was a limited number of small syncytia (fewer than 10 nuclei per syncytium); when SI was 2, there was an increase in both the size and number of syncytial foci per field; when SI was 3, there was extensive syncytium formation and coalescence of individual syncytial foci; when SI was 4, >90% of the monolayer was fused and beginning to detach from the substratum. Examples of the different syncytial indices are shown in Fig. 3 and 4.

Uridine release assay. Cell membrane integrity was assessed using a standard [^{3}H]uridine release assay commonly employed to analyze the membrane-lytic properties of viroporins (1, 4, 6, 9, 38). Twelve-well cluster plates of QM5 or Vero cells were incubated in the presence of 2 μCi/ml of [^{3}H]uridine (Sigma) for 18 h. The radiolabeled medium was removed, cells were washed three times with Hank's balanced salt solution, and cells were infected or transfected. At the indicated times, the cell monolayer and culture medium were harvested to determine the percent release of [^{3}H]uridine. The cell medium was removed, and the volume was adjusted to 1 ml with PBS and centrifuged at 1,500 × *g* for 5 min to pellet detached cells. The remaining cell monolayer was washed with PBS, incubated on ice in 200 μl of lysis buffer containing protease inhibitors (50 mM Tris-HCl, pH 8, 150 mM NaCl, 1 mM EDTA, 1% [vol/vol] Igepal [Sigma], 0.5% [wt/vol] sodium deoxycholate, 0.1% [wt/vol] sodium dodecyl sulfate [SDS], 200 nM aprotinin, 1 μM leupeptin, and 1 μM pepstatin) for 5 min, and then the volume was adjusted to 1 ml with PBS and added to the cell pellet from the previously removed medium. Samples (200 μl) were added to 1 ml of scintillation cocktail in duplicate, and radioactivity was quantified with a liquid scintillation counter. Control experiments involving the addition of lysis buffer or unlabeled cell lysates to culture medium containing [^{3}H]uridine determined that the efficiency of scintillation counting was the same under all conditions. The percent uridine release was determined by dividing the average counts per minute present in the culture medium by the total counts in the culture medium plus cell lysates. The labeling efficiency (total counts incorporated into cells) was approximately 1×10^5 cpm, and maximal release from syncytial cells corresponded to ~80% (~80,000 cpm).

Hygromycin B assay. At the indicated times posttransfection, cells were incubated for 45 min in methionine-free minimal essential medium with or without 1.5 mM of the membrane-impermeable translation inhibitor hygromycin B (Sigma). Cells were then labeled with 75 μCi/ml of [^{35}S]methionine for 45 min in the presence or absence of 1.5 mM hygromycin B. Labeled cells were washed three times with cold PBS and lysed for 2 min in 400 μl of cold lysis buffer. Nuclei and particulate cell debris were pelleted by centrifugation at 16,000 × *g* for 5 min. Lysates were collected and added to 100 μl of 5× protein sample buffer. Samples were subjected to SDS-polyacrylamide gel electrophoresis (10% acrylamide) and visualized using dimethyl sulfoxide-PPO (2,5-diphenyloxazole) fluorography as previously described (14).

DNA fragmentation assay. Semiconfluent monolayers of transfected QM5 cells were harvested at various times posttransfection with 10 mM EDTA in PBS. Cells were pelleted at 1,500 × *g* for 5 min and resuspended in 200 μl of PBS. DNA was isolated using the DNeasy DNA extraction kit (QIAGEN) as per the

manufacturer's instructions. Samples were subjected to agarose gel (1%, wt/vol) electrophoresis and visualized with 1% (wt/vol) ethidium bromide to detect DNA degradation in the form of nucleosomal laddering, a hallmark feature of apoptosis.

RESULTS

Avian reovirus induces late-stage alterations in membrane permeability. As an initial step to examine correlations between the rate and extent of syncytium formation, membrane leakiness, and virus release, we analyzed ARV-138, a small syncytium-inducing strain that exhibits limited pathogenicity in embryonated eggs. Transfer of the p10-encoding S1 genome segment from a highly fusogenic ARV strain to ARV-138 confers increased fusion potential (17), suggesting that the reduced fusogenic activity of ARV-138 relates to the p10 FAST protein. Membrane integrity was monitored using a standard [^{3}H]uridine release assay used extensively to characterize viroporin-induced changes in membrane permeability to small molecules (1, 4, 6, 9, 38, 47). QM5 cells were infected with ARV-138 (MOI = 5), and the release of [^{3}H]uridine and infectious progeny virus were assayed at various times postinfection (Fig. 2A). Cells infected in parallel were used to monitor the extent of syncytium formation by Giemsa staining (Fig. 2B). ARV-138 induced the formation of small syncytia at 9 h postinfection that slowly increased to include the majority of cells by approximately 20 h postinfection. Even at this late time point, and in spite of extensive syncytium formation, the extent of [^{3}H]uridine release did not exceed the level of spontaneous release from mock-infected cells (Fig. 2A), implying that the membrane integrity of the syncytia was not compromised. Significant uridine release did occur between 20 and 36 h postinfection (Fig. 2A) as syncytia progressed to encompass the entire monolayer and began to detach from the substratum (Fig. 2B). The increase in uridine release coincided with the release of infectious ARV-138 progeny virus particles (Fig. 2A), confirming previous reports that ARV induces late-stage alterations in membrane integrity and cell lysis (4, 15). However, the kinetics of membrane permeabilization induced by the weakly fusogenic ARV-138 were markedly delayed (20 to 36 versus 9 to 12 h postinfection) relative to the highly fusogenic ARV-176 and ARV-S1133 strains (4, 15), indicating correlations between the rate of ARV-induced polykaryon formation, membrane permeabilization, and virus release.

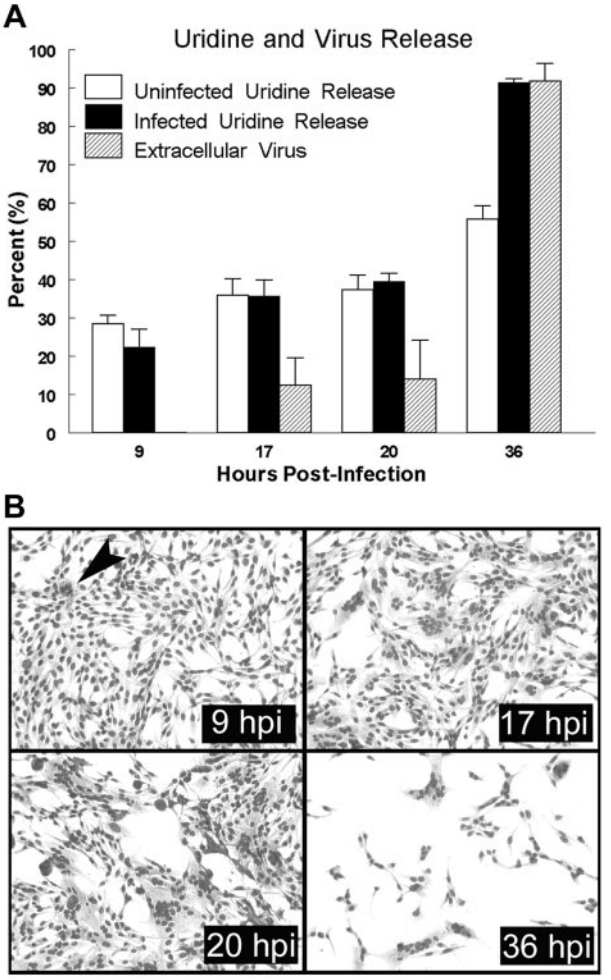

FIG. 2. Increased membrane permeability during late-stage avian reovirus infection correlates with virus release. (A) QM5 cells preloaded with [^{3}H]uridine were infected with ARV-138 (MOI = 5) and harvested at the indicated times postinfection. Percent uridine release from mock- and ARV-138-infected cells was quantified by scintillation counting, and the percent extracellular virus was determined by plaque assay. Results are expressed as the means ± standard deviations of a representative experiment conducted in triplicate. (B) Infected cells were fixed and Giemsa stained at the indicated times postinfection to detect syncytium formation. Images were captured by light microscopy at ×100 magnification. The arrow indicates an early syncytium.

The extent of p10-mediated syncytium formation correlates with the rate of small-molecule efflux. To directly examine the relationship between FAST protein-mediated syncytium formation and membrane alterations, we examined the kinetics of syncytium formation and increased membrane permeability in transfected cells expressing the related ARV or NBV p10 protein. Syncytium formation was assessed by microscopic observation of Giemsa-stained monolayers, and an SI was assigned by qualitatively scoring, on a scale from 0 to 4, the relative extent of cell fusion (Fig. 3B). Although ARV and NBV p10 share 33% amino acid identity and contain the same repertoire and arrangement of structural motifs (Fig. 1), they displayed dramatically different fusion kinetics. By 12 to 14 h posttransfection, cells expressing NBV p10 were extensively fused (SI = 3), and by 16 to 18 h, the entire monolayer was fused and beginning to detach from the substratum (Fig. 3A, right panel, and B). In contrast, ARV p10-transfected cells took 24 to 36 h to reach an SI of 3, 48 h before the entire monolayer was fused (Fig. 3A, left panel). The basis for the different fusion kinetics of these two versions of p10 is unknown but is under investigation.

The kinetics of uridine release correlated with the relative rates of syncytium formation induced by these p10 homologues, with altered membrane permeability ensuing only well after extensive syncytium formation. For example, ARV p10-induced uridine release barely exceeded the level of spontaneous release from mock-transfected cells by 36 h posttransfection, at which point the monolayer had already been extensively fused for approximately 12 h (Fig. 3A, left panel), and uridine release was not statistically significant ($P < 0.01$) until 48 h posttransfection. The same trend (i.e., no significant uridine release until well after syncytium formation was extensive)

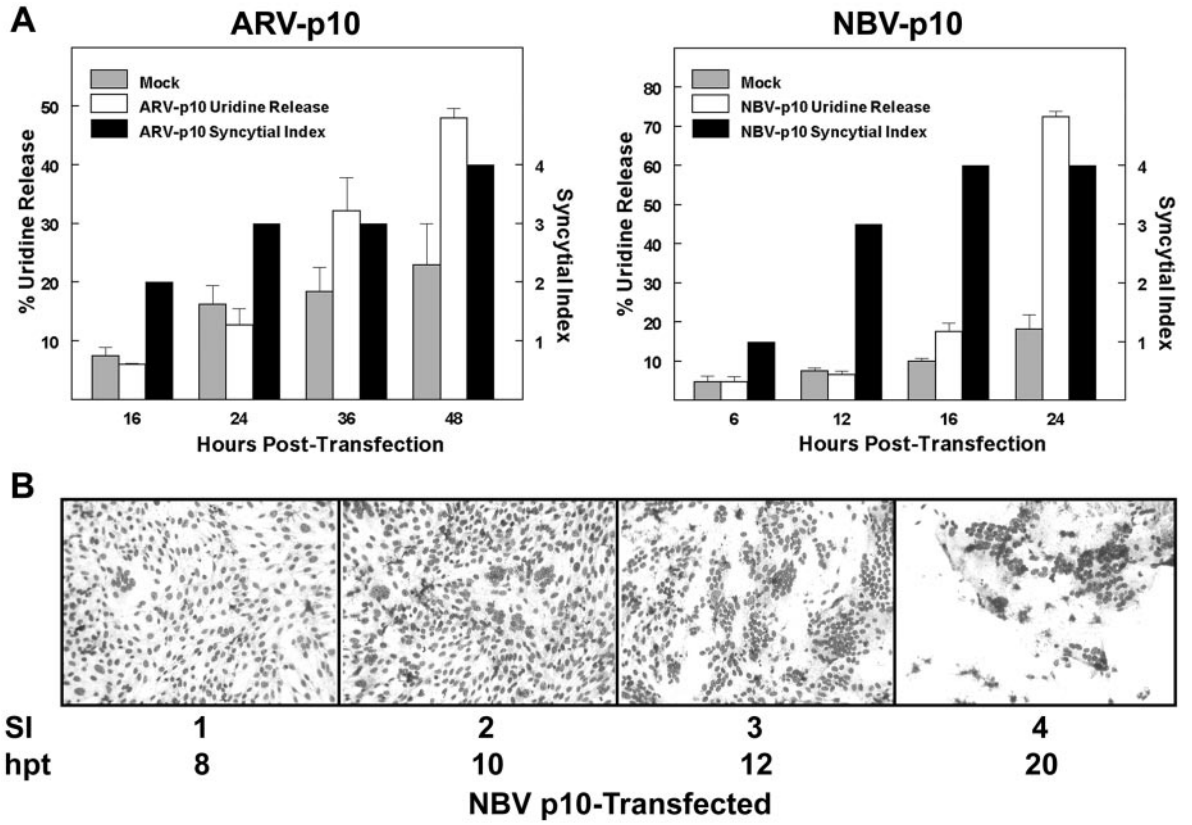

FIG. 3. Syncytium formation induced by the p10 FAST proteins results in increased late-stage membrane permeability. (A) QM5 cells were labeled with [^{3}H]uridine prior to transfection with the control plasmid (mock) or with plasmids expressing the NBV p10 or ARV p10 FAST protein. At the indicated times posttransfection, the percent uridine release was quantified by scintillation counting. Data are presented as the means ± standard errors of three independent experiments. At the same time points, parallel Giemsa-stained monolayers were observed by light microscopy and qualitatively scored for the extent of syncytium formation on a scale of 0 to 4. (B) Light microscopy images (×80 magnification) of Giemsa-stained monolayers transfected with the NBV p10 expression plasmid at various times (hours) posttransfection (hpt). The SI at each time point is indicated and corresponds to the results presented in panel A. The same procedure was used to determine the SI of ARV p10.

was observed in NBV p10-transfected cells but with different kinetics. By 12 h posttransfection, the majority of cells in NBV p10-transfected monolayers were involved in syncytia, with no evidence of increased uridine release. By 16 h posttransfection, when the entire monolayer was fused, uridine release was minimal, though statistically significant ($P < 0.005$) (Fig. 3A, right panel, and B). Uridine leakage from NBV p10-transfected cells reached maximal levels by 20 to 24 h posttransfection, coinciding with the destruction of the cell monolayer. Therefore, as with ARV-infected cells, a correlation between the rate and extent of syncytium formation induced by the p10 FAST proteins and membrane leakage existed.

Altered membrane integrity is a generalized feature of FAST protein-mediated syncytium formation. To determine whether the rate of syncytium formation mediated by other members of the FAST protein family also correlated with altered membrane permeability, we examined RRV p14 and BRV p15 using the same assays. RRV p14-transfected cells displayed remarkably rapid fusion kinetics in QM5 cells, with polykaryons appearing as early as 4 to 6 h posttransfection (Fig. 4A, right panel). Uridine release, however, was not detected until 16 h posttransfection, approximately 4 h after the majority of cells in the monolayer were fused and syncytia began detaching from the substratum (Fig. 4A). In contrast, p15 induced syncytium formation at a very slow rate, with polykaryons not appearing until 13 to 16 h posttransfection (Fig. 4A, left panel, and B). As a result of the slow rate of cell fusion, p15-induced syncytium formation did not exceed an SI of 3 by the conclusion of the experiment at 48 h posttransfection. Uridine leakage from p15-transfected cells did not reach statistically significant levels above spontaneous release from mock-transfected cells, although a trend of increased uridine release was noted between 36 and 48 h posttransfection (Fig. 4A). Therefore, the extent of altered membrane permeability induced by all members of the FAST protein family, as inferred from increased small-molecule release from syncytial cells, correlated with the respective ability of each FAST protein to mediate multinucleated syncytium formation in cell culture. We are unsure of the basis behind the different fusion kinetics of the various FAST proteins, but it may reflect differences in protein expression and/or stability.

Extensive syncytium formation is a requirement for membrane leakage. To determine whether the observed correlation between FAST protein-induced syncytium formation and membrane leakage reflected a causal relationship, we designed two experiments to test whether altered membrane permeability was due to cell-cell fusion or some syncytium-independent influence of the FAST proteins. In the first study, we exploited

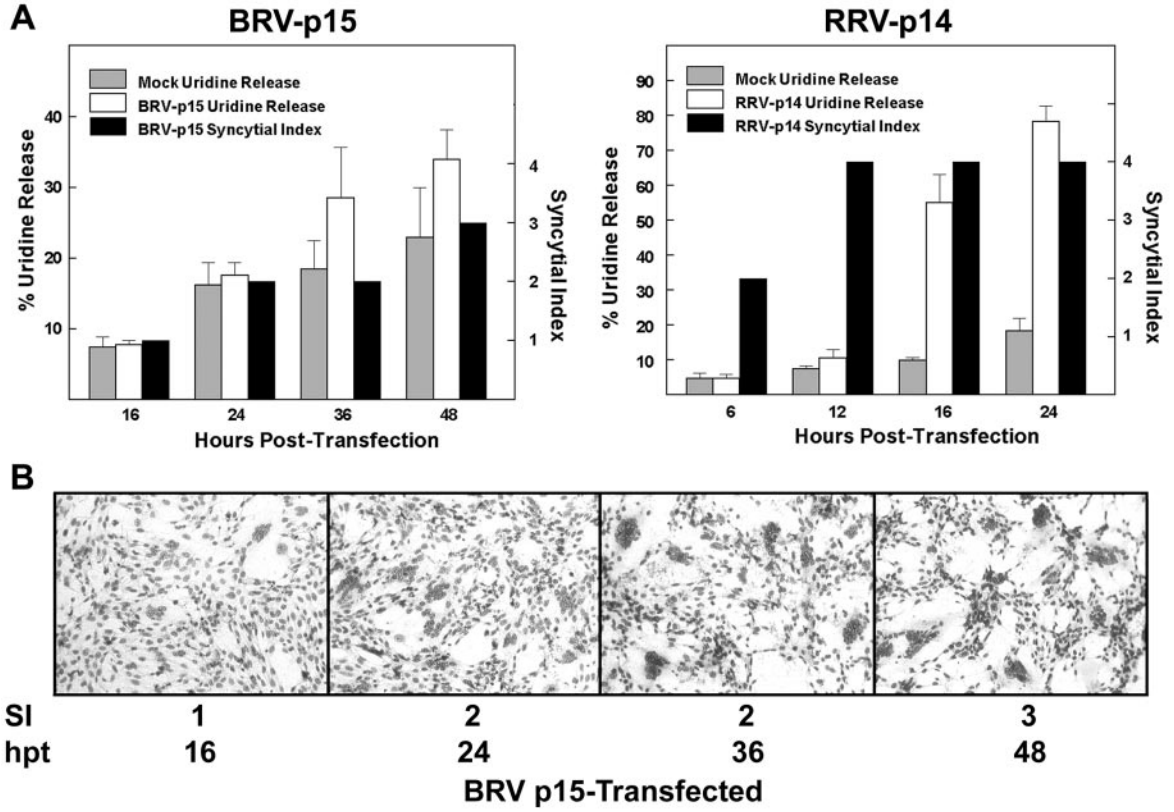

FIG. 4. Membrane permeability changes induced by the BRV p15 and RRV p14 FAST proteins. (A) QM5 cells were labeled with [^{3}H]uridine prior to transfection with the control plasmid (mock) or with plasmids expressing the BRV p15 or RRV p14 FAST protein. At the indicated times posttransfection, the percent uridine release was quantified by scintillation counting. Data are presented as the means ± standard errors of three independent experiments. The syncytial index was determined at the same time points, as described in the legend of Fig. 3. (B) Light microscopy images (×80 magnification) of Giemsa-stained monolayers transfected with the BRV p15 expression plasmid at various times (hours) posttransfection (hpt). The SI at each time point is indicated. The same procedure was used to determine the SI of RRV p14.

the ability of a polyclonal anti-p14 antiserum to inhibit p14-mediated syncytium formation (12). The effect of this antibody inhibition of cell-cell fusion on membrane permeability was assessed by the uridine release assay. At 20 h posttransfection, p14-transfected cells treated exogenously with anti-p14 were severely restricted in their ability to generate syncytia (SI = 1) with a concomitant inhibition of uridine release. Control cells, transfected with p14 and treated with normal rabbit serum, displayed both extensive syncytium formation and uridine leakage (Fig. 5A). In the second approach, we utilized a nonfusogenic ARV p10 construct containing a deletion of the N-terminal 24 residues (p10del). This p10 construct retains the integral membrane nature of authentic p10 but is devoid of membrane fusion activity (53). Contrary to a previous report in BSC-40 cells (4), p10del failed to induce altered membrane integrity above control levels in QM5 cells (Fig. 5B). The use of both antisera and fusion-minus FAST protein constructs to prevent syncytium formation provided compelling evidence that the observed alterations in membrane stability result from extensive syncytium formation and not the mere presence of the FAST proteins in the plasma membrane.

Syncytium-induced membrane leakage is bidirectional. The analysis of membrane leakage from FAST protein-induced syncytia by monitoring uridine efflux was confirmed by examining the sensitivity of syncytial cells to influx of another small molecule, hygromycin B. Hygromycin B is a translation inhibitor, similar in size to uridine, and normally membrane impermeable (8, 9). When membrane stability is altered, hygromycin B entry into cells is detected by a global decrease in cellular translation. This assay is commonly employed to analyze viroporin activity (8, 26). As with mock-transfected cells, NBV p10-transfected cells were insensitive to hygromycin B at early times posttransfection (12 h), when syncytium formation had progressed to an SI of 2 to 3, confirming the membrane-impermeant nature of the inhibitor (Fig. 6A). By 20 h posttransfection, when the NBV-transfected cells reached an SI of 3 to 4, cells became sensitive to hygromycin B, as evidenced by a global decrease in translation levels. These results were in close agreement with the uridine leakage data, indicating that the permeability of syncytial cell membranes to both efflux and influx of small molecules was not compromised until syncytium formation was extensive.

The same situation applied to p14-transfected cells, although with different kinetics, where an SI of 4 was reached by 12 h posttransfection, at which time cells were sensitive to hygromycin B treatment (Fig. 6B). We also observed a decrease in cellular translation in extensively fused, RRV p14-transfected cells that were not treated with hygromycin B compared to that in mock-transfected cells which was likely due to cell death or detachment associated with extensive syncytium for-

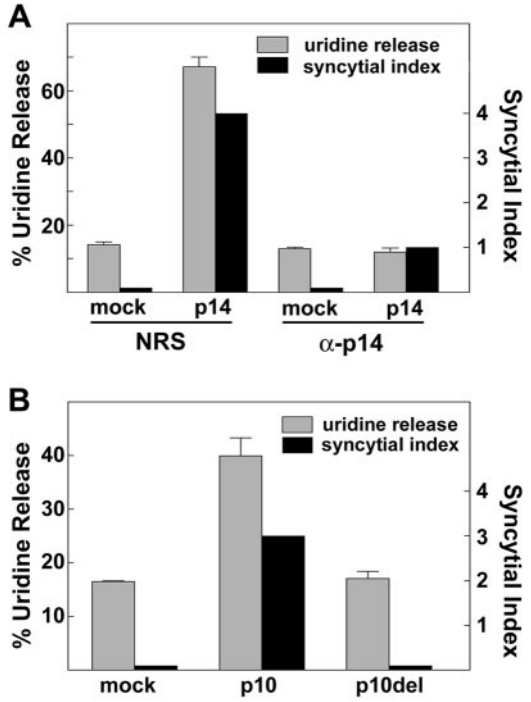

FIG. 5. Inhibition of syncytium formation prevents membrane permeabilization. (A) QM5 cells were labeled with [^{3}H]uridine prior to transfection with the empty vector (mock) or with the RRV p14 expression vector. At 3 h posttransfection, anti-p14 polyclonal antiserum (α-p14) or normal rabbit serum (NRS) was added to cells (1:20 dilution). The percent uridine release and syncytial index were determined at 20 h posttransfection, as described in the legend of Fig. 3. Values represent the means ± standard deviations of a representative experiment conducted in triplicate. (B) QM5 cells were labeled with [^{3}H] uridine prior to transfection with the empty vector (mock), with a plasmid vector expressing the authentic ARV p10 protein (p10), or with a plasmid expressing a nonfusogenic N-terminally-truncated version the ARV p10 protein (p10-del). The percent uridine release and syncytial index were determined at 48 h posttransfection, as described in the legend of Fig. 3. Values represent the means ± standard deviations of a representative experiment conducted in triplicate.

mation. As with the uridine release assay, the addition of anti-p14 to prevent p14-mediated fusion also eliminated the sensitivity of cells to hygromycin B (Fig. 6B). Moreover, these observations were not cell specific, as RRV p14-mediated syncytium formation resulted in hygromycin B sensitivity that correlated with extensive fusion when the assay was performed in Vero cells (Fig. 6C). As with the QM5 cells, Vero cells that were extensively fused (SI approaching 3), for example, by NBV p10 at 19 h posttransfection, revealed little hygromycin B sensitivity (Fig. 6C). Thus, the altered membrane permeability associated with FAST protein expression is dependent on extensive FAST-mediated syncytium formation.

Extensive syncytium formation results in an apoptotic response. Our analysis revealed that the consequence of FAST protein-induced cell-cell fusion is the ultimate detachment and death of the syncytial cells. To explore the nature of the loss of syncytial cell viability, we analyzed the large syncytia induced by RRV p14 for indicators of apoptosis. RRV p14-transfected cells were fixed at 24 h posttransfection (SI = 4), and nuclei were stained with DAPI (4′,6′-diamidino-2-phenylindole), a fluorescent dye used to detect the chromatin condensation associated with cells undergoing apoptosis (5, 25, 34). Mock-transfected cells displayed a few occasional cells with fluorescent nuclei suggestive of condensed chromatin and apoptosis, and syncytia present in p14-transfected cells demonstrated numerous pyknotic nuclei with condensed chromatin (Fig. 7A). Interestingly, some syncytia contained almost entirely nuclei with condensed chromatin, while few of the nuclei in other syncytia demonstrated chromatin condensation, suggesting that an apoptotic response, once triggered in a syncytium, rapidly proceeds to affect all nuclei in that syncytium.

To confirm the DAPI results implicating an apoptotic response in the destruction of syncytial cells, we analyzed FAST protein-transfected cells for oligonucleosomal DNA fragmentation, a hallmark feature of apoptosis (30, 42, 43). Chromosomal DNA was isolated from RRV p14- and NBV p10-transfected cells at various times posttransfection and analyzed for DNA fragmentation by agarose gel electrophoresis and ethidium bromide staining (Fig. 7B). In both cases, no DNA degradation was apparent by 12 h posttransfection at an SI of 3 but

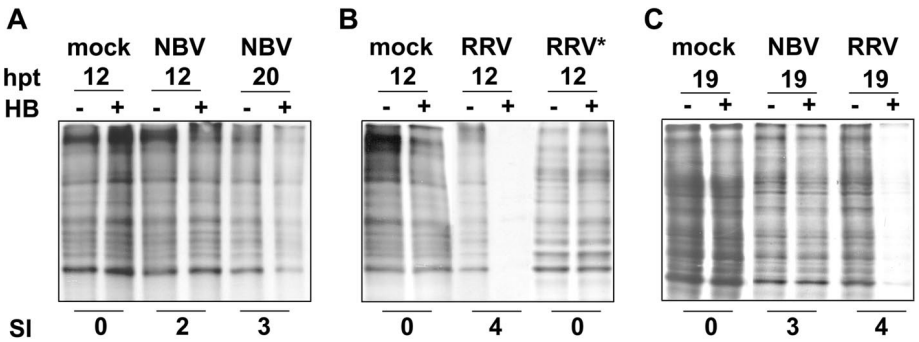

FIG. 6. Membrane permeabilization is bidirectional and not cell specific. QM5 (panels A and B) or Vero cells (panel C) were transfected with empty vector (mock) or with vectors expressing the RRV p14 or NBV p10 FAST protein. At the indicated times (hours) posttransfection (hpt), cells were incubated in methionine-free medium in the absence or presence of 1.5 mM hygromycin B for 45 min and then pulse-labeled with [^{35}S] methionine with or without hygromycin B for 45 min. Cells were lysed in radioimmunoprecipitation buffer, and radiolabeled cell proteins were resolved by SDS-polyacrylamide gel electrophoresis (15% acrylamide) and detected by autoradiography to assess the relative degree of translation in cells. The SI at the time of labeling was determined by Giemsa staining and light microscopy, as described in the legend of Fig. 3. RRV* denotes RRV p14-transfected cells treated with anti-p14 antibody to inhibit fusion, as described in the legend of Fig. 5.

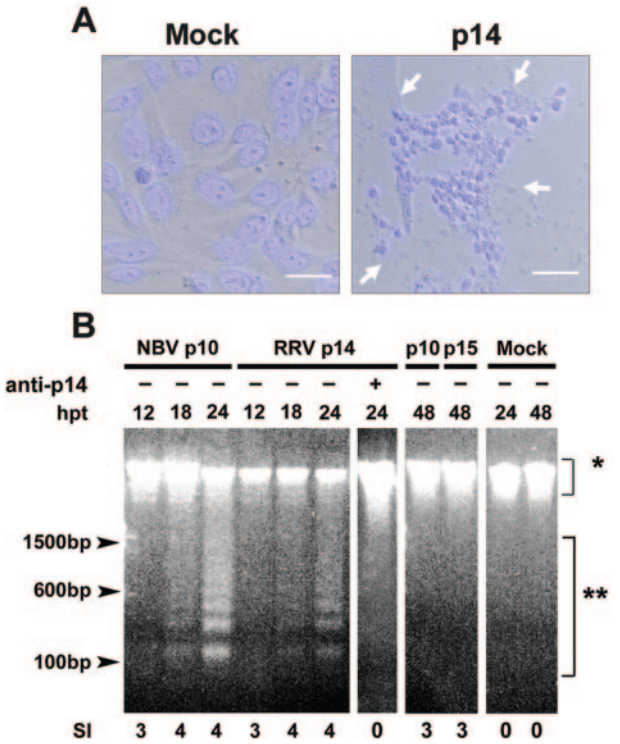

FIG. 7. FAST-mediated syncytium formation triggers apoptosis. (A) QM5 cells transfected with empty vector (mock) or an RRV p14 expression vector were fixed at 24 h posttransfection and stained with DAPI. Arrows in the right panel indicate the edges of a single syncytium containing a cluster of pyknotic nuclei. Scale bar = 10 μm. (B) DNA was isolated from mock-transfected cells or from transfected cells expressing the indicated FAST proteins at various times (hours) posttransfection (hpt). One of the p14-transfected samples was incubated with anti-p14 antiserum to inhibit syncytium formation, as described in the legend of Fig. 5. Isolated DNA was resolved on 1% agarose gels. The locations of intact (*) and oligonucleosomal DNA fragments (**) are indicated on the right. The locations of DNA size markers are indicated on the left. The SI at the time of DNA isolation was determined as described in the legend of Fig. 3 and is indicated for each sample.

became detectable by 18 h posttransfection and obvious by 24 h posttransfection as indicated by the appearance of oligonucleosomal laddering. DNA fragmentation occurred at approximately the same time as uridine release (Fig. 3 and 4) and appeared to be dependent on extensive cell-cell fusion, as antibody inhibition of p14-mediated syncytium formation eliminated DNA fragmentation (Fig. 7B). ARV p10- and BRV p15-transfected cells, which in this experiment had reached an SI of only 3 by 48 h posttransfection, failed to induce detectable DNA fragmentation. Therefore, the FAST protein-mediated induction of extensive syncytium formation coincides with a loss of membrane integrity and an apoptotic response.

The apoptotic response is responsible for altered membrane integrity. The kinetics of membrane leakage and chromatin condensation and degradation did not permit an assessment of whether membrane leakage triggers an apoptotic response or whether syncytium-induced activation of apoptotic pathways results in alterations in membrane integrity. To distinguish between these two possibilities, we examined the effects of the cell-permeant broad-spectrum caspase inhibitor Z-VAD-fmk on membrane leakage. Addition of the caspase inhibitor to p14-transfected cells had no effect on p14-induced syncytium formation (Fig. 8C) but had a dramatic effect on [^{3}H]uridine leakage (Fig. 8A). By 18 h posttransfection, monolayers that were not treated with the apoptosis inhibitor and which had already been at an SI of 4 for 4 h displayed the oligonucleosomal laddering characteristic of apoptotic cells (Fig. 8B). Coincident with the appearance of chromatin degradation, extensive uridine leakage occurred from untreated p14-transfected cells (Fig. 8A). The addition of Z-VAD-fmk to transfected cells prevented chromatin degradation (Fig. 8B), consistent with the ability of this inhibitor to prevent caspase-activated, DNase-mediated oligonucleosomal DNA cleavage (56). The apoptotic inhibitor also eliminated uridine leakage from cells (Fig. 8A) in spite of the fact that the entire monolayer had fused into one giant syncytium (Fig. 8C). We therefore conclude that extensive syncytium formation results in apoptosis-induced alterations to membrane integrity and cell death.

DISCUSSION

The unusual ability of nonenveloped viruses to induce cell-cell fusion is associated solely with several members of the family *Reoviridae*. Recent reports clearly indicate the role of the FAST protein family in reovirus-induced syncytium formation (4, 12, 14, 53). However, little is known in regard to how these proteins induce membrane fusion or why nonenveloped viruses would encode such proteins. We now show that the mechanism of FAST protein-induced membrane fusion is a relatively nonleaky process. All of the FAST proteins do, however, induce alterations to membrane permeability. This is not the result of a porin or lytic activity associated with the FAST proteins but instead reflects a cellular response to FAST-induced syncytium formation that results in apoptosis-mediated effects on membrane stability. These observations have relevance to proposed models of the possible role of the FAST proteins in virus-host interactions.

The FAST proteins function as membrane fusion proteins, not viroporins. The FAST proteins bear no resemblance to typical viral membrane fusion proteins that are relatively large, multimeric structural proteins with complex ectodomain structures (27, 55). Similarities do exist, however, between the FAST proteins and a broad class of viral proteins that perturb host membranes, the viroporins. Viroporins are typically small, integral membrane proteins with membrane-proximal polybasic domains. Examples include the human immunodeficiency virus (HIV) Vpu, influenza M2, and picornavirus 3A and 2B proteins as well as two viroporins encoded by genera within the family *Reoviridae*, the rotavirus NSP4 and the orbivirus NS3 proteins (6, 26, 60). In addition to their structural features, viroporins share the functional property of altering membrane permeability to ions and small molecules such as uridine and hygromycin B and have been implicated in virus-induced cytopathic effects and in facilitating virus release (8, 9, 26, 41).

Recently, ARV p10 was reported to cause membrane destabilization, leading to the proposal that p10 is a reovirus viroporin (4). Moreover, a fusion-minus construct of p10 induced membrane leakage from transfected BSC-40 cells, suggesting that p10-induced membrane leakage is not dependent on

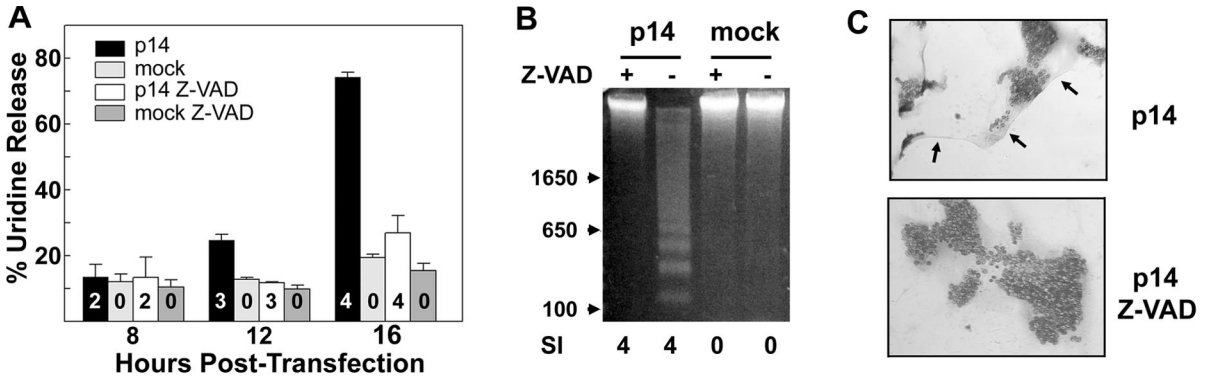

FIG. 8. Inhibiting caspase activity inhibits increased membrane permeability. (A) QM5 cells were labeled with [^{3}H]uridine prior to transfection with the empty vector (mock) or with the RRV p14 expression vector. Cells were incubated in the absence or presence of the pancaspase inhibitor Z-Vad-fmk. The percent uridine release was determined at the indicated times posttransfection, as described in the legend of Fig. 3. Values represent the means ± standard deviations of a representative experiment conducted in triplicate. Numbers within each histogram indicate the syncytial index of each sample at that time point, determined as described in the legend of Fig. 3. (B) DNA was isolated from mock-transfected or p14-transfected cells at 16 h posttransfection. Isolated DNA was resolved on 1% agarose gels. The locations of DNA size markers are indicated on the left. The SI at the time of DNA isolation was determined as described in the legend of Fig. 3 and is indicated for each sample. (C) Cells expressing p14 in the absence or presence of Z-Vad-fmk were fixed and Giemsa stained at 16 h posttransfection, at which time the entire monolayer was fused and contained large clusters of nuclei present in a continuous syncytium. Arrows in the left panel indicate the edges of the syncytium detaching from the substratum.

membrane fusion. It was also stated that these two events are not concurrent, with membrane permeabilization always preceding syncytium formation (4). These observations suggested that the primary function of p10 is to destabilize cell membranes. If so, perhaps the FAST proteins evolved from a viroporin that possesses the ability to destabilize the donor membrane to a fusion protein that can destabilize both donor and target membranes sufficiently to effect membrane merger. This speculation is not unreasonable, as evidenced by the recent demonstration that the VP5 protein of bluetongue virus, a nonenveloped virus capsid protein involved in endosomal membrane permeabilization, is capable of causing cell-cell fusion when modified to include a signal peptide and a transmembrane domain (22). Though an intriguing theory, our data suggest otherwise. All four FAST proteins were capable of inducing extensive syncytium formation in the absence of any indication of altered membrane permeability to efflux or influx of small molecules. Alterations to membrane stability occurred only well after syncytia were extensive in QM5 fibroblast or Vero cells and did not occur when FAST proteins were expressed but cell-cell fusion was inhibited, either by use of a fusion-minus p10 construct or by antibody inhibition of p14-induced syncytium formation. Other fusion-inactive ARV p10 constructs gave similar results, as did membrane permeability assays based on DAPI or trypan blue staining or on ^{51}Cr release (data not shown). Therefore, in our hands, FAST-induced syncytium formation was a prerequisite for, and always preceded, membrane leakage. This observation argues against FAST protein-induced syncytium formation being the consequence of viroporin-like membrane disruption. It is possible that the FAST proteins may possess some membrane-destabilizing activity under certain conditions, such as in *Escherichia coli* or BSC-40 cells (4). However, our results indicate that the FAST proteins are capable of orchestrating the reorganization of lipid bilayers in such a manner so as not to alter the membrane permeability barrier, suggesting that the FAST proteins have evolved specifically as membrane fusion proteins.

FAST protein-induced syncytium formation triggers an apoptotic response that contributes to altered membrane integrity. Although cell-cell fusion is an uncommon property of nonenveloped viruses, syncytium formation is associated with the replication cycle of numerous enveloped viruses, reflecting the presence of viral fusion proteins in the plasma membrane of virus-infected cells, a natural consequence of the assembly and release strategies of these viruses. While it is generally accepted that virus-induced syncytium formation is a nonphysiological process that contributes to cytopathic effects, the mechanism of syncytial death remains a matter of debate. For example, numerous studies disagree as to whether syncytia induced by measles virus or HIV undergo apoptotic or necrotic cell death (2, 10, 19–21, 23, 46, 51). Our results indicate that FAST protein-induced syncytial cells died in a manner characteristic of apoptosis. Syncytial nuclei revealed morphological changes indicative of apoptosis, such as chromatin condensation and marginalization, which were apparent only in large syncytia at late transfection times (Fig. 7A). Moreover, oligonucleosomal DNA laddering (a hallmark indicator of apoptosis) was observed in FAST-transfected cells at late transfection times, laddering only occurred after syncytium formation was extensive (Fig. 7B), and DNA degradation was prevented by the pancaspase inhibitor Z-VAD-fmk (Fig. 8). Similar observations have been reported for lentivirus-induced syncytium formation where apoptotic cell death is inhibited by Z-VAD-fmk (10, 18, 51), while the necrotic cell death attributed to syncytia induced by the gibbon ape leukemia virus fusion protein shows no such inhibition (29). We therefore conclude that FAST-induced syncytium formation triggers an apoptotic cell response.

Results further indicated that membrane leakage was a consequence of the syncytium-triggered apoptotic response. The ability of a caspase inhibitor to prevent both DNA degradation

and uridine leakage (Fig. 8) provided compelling evidence of a causal relationship between apoptosis and membrane leakage. The inhibitor had no effect on p14-induced syncytium formation that progressed to encompass the entire monolayer, in effect generating a single syncytium with $>10^6$ nuclei that displayed no loss in membrane integrity. This was a dramatic demonstration that FAST-induced cell-cell fusion is a relatively nonleaky process, that the FAST proteins do not display syncytium-independent membrane-lytic properties in eukaryotic cells, and that a syncytium-triggered apoptotic response directly contributes to altered membrane integrity and disruption of syncytia.

These results contrast markedly with studies of the physiological syncytium formation that occurs during such cellular processes as the formation of syncytiotrophoblasts, myotubes, and osteoclasts (32, 48, 49, 58). In these cases of virus-independent syncytium formation, cell-cell fusion is the result of specific differentiation pathways. Evidence suggests that cell fusion is actually dependent on triggering early stages of the apoptotic cascade, including activation of the initiator caspase 8 and externalization of phosphatidylserine (3, 31, 58). Subsequent to syncytial fusion, progression of the apoptosis cascade is retarded, in part by expression of the antiapoptotic Bcl-2 protein throughout the syncytiotrophoblast, while localized expression of the proapoptotic Bak protein has been implicated in regulated turnover and maintenance of the syncytium (31, 32, 48, 49). In the case of virus-induced syncytium formation, the apoptotic response is likely triggered in a nonspecific manner rather than by regulated initiation of apoptotic pathways. Such proapoptotic signals could involve altered cell homeostasis due to gross changes in cytoskeletal arrangement and/or surface/volume ratios that presumably accompany syncytium formation or by acquiring a dominant apoptotic signal via incorporation of cells undergoing spontaneous apoptosis into the growing syncytium (51). Our kinetic analysis indicates that whatever the signal, there is a significant lag between FAST protein-induced polykaryon formation and the effects of triggering the apoptotic response. As a result, syncytial cells remain viable and metabolically active until late in the infection cycle. Some viruses have been shown to use apoptosis as a means to spread to adjacent cells, providing the process is not triggered too early in the replication cycle (45).

Potential dual role for syncytium formation in the virus replication cycle. Although syncytium formation is well described in enveloped viruses, the influence of cell-cell fusion on the virus replication cycle and viral pathogenesis remains unclear. In the case of HIV, transition from a nonsyncytial to syncytium-inducing phenotype correlates with advanced disease progression (7, 35, 50). Since the change in syncytial phenotype corresponds to changes in gp120, however, it is difficult to separate the effects of altered coreceptor utilization and cell tropism from the influence of syncytium formation. In other instances, such as measles virus, a clearer case can be made for syncytium formation serving as a pathogenic determinant, where increased pathogenicity correlates with the presence of syncytial phenotype even in the presence of reduced viral titers (11). It is assumed that enhanced pathogenicity reflects increased lateral cell-cell spread of the infection.

There is evidence to suggest that the FAST proteins may function as virulence factors. Unlike the prototypical mammalian reoviruses which are nonfusogenic and relatively benign, the fusogenic reoviruses induce a variety of clinical symptoms following natural infections (40, 44, 57, 61). Syncytium formation has also been detected by histopathological examination of tissues from animals infected with fusogenic reoviruses (28, 36, 37, 39, 61). Furthermore, a comparative study of two different strains of ARV revealed a correlation between the extent of syncytium formation and viral pathogenesis (17). There are, therefore, several correlates that suggest that reovirus-induced syncytium formation functions as a virulence factor.

We previously proposed that enhanced virus release due to syncytial lysis might contribute to the pathogenic potential of ARV (17). Based on our present results, we suggest that syncytium formation may serve an additional role in the virus replication cycle by first promoting localized in vivo establishment of the infection via lateral cell-cell transmission. Since membrane integrity is maintained throughout the early stages of the fusion process (Fig. 3 to 6), infected cells remain viable, allowing the virus to access the translational machinery of adjacent cells without having to invoke scenarios where virus translation can proceed in the presence of altered intracellular ion concentrations. In addition, the virus would be able to evade the host immune defense until a localized infection is well established. Following a robust localized infection and concomitant with the development of extensive syncytia, apoptosis-induced alterations in membrane permeability would facilitate more efficient virus release allowing systemic dissemination of the infection, as shown here for ARV-138 (Fig. 2) and as previously shown for ARV-176 (15). Support for this proposal is derived from previous results indicating that in the absence of syncytium formation, ARV remains cell associated until syncytium-independent virus-induced cytopathic effects trigger delayed virus release (15). Further in vivo validation of this model with a fusion-deficient avian reovirus isolate awaits the development of a reverse genetics system for the fusogenic reoviruses. Regardless of the actual role of syncytium formation in the replication cycle and pathogenicity of the fusogenic reoviruses, it seems clear that all of these viruses have evolved to maintain a small integral membrane protein that functions as a dedicated membrane fusion protein.

ACKNOWLEDGMENTS

We thank Jennifer Corcoran for her insightful comments and critical reading of the manuscript and Jingyun Shou for excellent technical assistance.

This research was supported by grants from the Canadian Institutes of Health Research (CIHR). J.S. was funded by scholarships from the Natural Sciences and Engineering Research Council of Canada (NSERC) and from Cancer Research and Education, Nova Scotia (CaRE). D.T. was funded by a scholarship from CaRE. R.D. is the recipient of a CIHR-RPP Investigators award.

REFERENCES

1. **Aldabe, R., A. Barco, and L. Carrasco.** 1996. Membrane permeabilization by poliovirus proteins 2B and 2BC. J. Biol. Chem. **271:**23134–23137.
2. **Bateman, A. R., K. J. Harrington, T. Kottke, A. Ahmed, A. A. Melcher, M. J. Gough, E. Linardakis, D. Riddle, A. Dietz, C. M. Lohse, S. Strome, T. Peterson, R. Simari, and R. G. Vile.** 2002. Viral fusogenic membrane glycoproteins kill solid tumor cells by nonapoptotic mechanisms that promote cross presentation of tumor antigens by dendritic cells. Cancer Res. **62:**6566–6578.
3. **Black, S., M. Kadyrov, P. Kaufmann, B. Ugele, N. Emans, and B. Huppertz.** 2004. Syncytial fusion of human trophoblast depends on caspase 8. Cell Death Differ. **11:**90–98.

4. **Bodelon, G., L. Labrada, J. Martinez-Costas, and J. Benavente.** 2002. Modification of late membrane permeability in avian reovirus-infected cells: viroporin activity of the S1-encoded nonstructural p10 protein. J. Biol. Chem. **277:**17789–17796.
5. **Bojarski, C., A. H. Gitter, K. Bendfeldt, J. Mankertz, H. Schmitz, S. Wagner, M. Fromm, and J. D. Schulzke.** 2001. Permeability of human HT-29/B6 colonic epithelium as a function of apoptosis. J. Physiol. **535:**541–552.
6. **Browne, E. P., A. R. Bellamy, and J. A. Taylor.** 2000. Membrane-destabilizing activity of rotavirus NSP4 is mediated by a membrane-proximal amphipathic domain. J. Gen. Virol. **81:**1955–1959.
7. **Camerini, D., H.-P. Su, G. Gamez-Torre, M. L. Johnson, J. A. Zack, and I. S. Y. Chen.** 2000. Human immunodeficiency virus type 1 pathogenesis in SCID-hu mice correlates with syncytium-inducing phenotype and viral replication. J. Virol. **74:**3196–3204.
8. **Carrasco, L.** 1995. Modification of membrane permeability by animal viruses. Adv. Virus Res. **45:**61–112.
9. **Carrasco, L., M. J. Otero, and J. L. Castrillo.** 1989. Modification of membrane permeability by animal viruses. Pharmacol. Ther. **40:**171–212.
10. **Castedo, M., K. F. Ferri, J. Blanco, T. Roumier, N. Larochette, J. Barretina, A. Amendola, R. Nardacci, D. Metivier, J. A. Este, M. Piacentini, and G. Kroemer.** 2001. Human immunodeficiency virus 1 envelope glycoprotein complex-induced apoptosis involves mammalian target of rapamycin/FKBP12-rapamycin-associated protein-mediated p53 phosphorylation. J. Exp. Med. **194:**1097–1110.
11. **Cathomen, T., B. Mrkic, D. Spehner, R. Drillien, R. Naef, J. Pavlovic, A. Aguzzi, M. A. Billeter, and R. Cattaneo.** 1998. A matrix-less measles virus is infectious and elicits extensive cell fusion: consequences for propagation in the brain. EMBO J. **17:**3899–3908.
12. **Corcoran, J. A., and R. Duncan.** 2004. Reptilian reovirus utilizes a small type III protein with an external myristylated amino terminus to mediate cell-cell fusion. J. Virol. **78:**4342–4351.
13. **Corcoran, J. A., R. Syvitski, D. Top, R. M. Epand, R. F. Epand, D. Jakeman, and R. Duncan.** 2004. Myristoylation, a protruding-loop, and structural plasticity are essential features of a nonenveloped virus fusion peptide motif. J. Biol. Chem. **279:**51386–51394
14. **Dawe, S., and R. Duncan.** 2002. The S4 genome segment of baboon reovirus is bicistronic and encodes a novel fusion-associated small transmembrane protein. J. Virol. **76:**2131–2140.
15. **Duncan, R., Z. Chen, S. Walsh, and S. Wu.** 1996. Avian reovirus-induced syncytium formation is independent of infectious progeny virus production and enhances the rate, but is not essential, for virus-induced cytopathology and virus egress. Virology **224:**453–464.
16. **Duncan, R., J. Corcoran, J. Shou, and D. Stoltz.** 2004. Reptilian reovirus: a new fusogenic orthoreovirus species. Virology **319:**131–140.
17. **Duncan, R., and K. Sullivan.** 1998. Characterization of two avian reoviruses that exhibit strain-specific quantitative differences in their syncytium-inducing and pathogenic capabilities. Virology **250:**263–272.
18. **Duval, R., V. Bellet, S. Delebassee, and C. Bosgiraud.** 2002. Implication of caspases during maedi-visna virus-induced apoptosis. J. Gen. Virol. **83:**3153–3161.
19. **Esolen, L. M., S. W. Park, J. M. Hardwick, and D. E. Griffin.** 1995. Apoptosis as a cause of death in measles virus-infected cells. J. Virol. **69:**3955–3958.
20. **Ferri, K. F., E. Jacotot, J. Blanco, J. A. Este, N. Zamzami, S. A. Susin, Z. Xie, G. Brothers, J. C. Reed, J. M. Penninger, and G. Kroemer.** 2000. Apoptosis control in syncytia induced by the HIV type 1-envelope glycoprotein complex: role of mitochondria and caspases. J. Exp. Med. **192:**1081–1092.
21. **Ferri, K. F., E. Jacotot, P. Leduc, M. Geuskens, D. E. Ingber, and G. Kroemer.** 2000. Apoptosis of syncytia induced by the HIV-1-envelope glycoprotein complex: influence of cell shape and size. Exp. Cell Res. **261:**119–126.
22. **Forzan, M., C. Wirblich, and P. Roy.** 2004. A capsid protein of nonenveloped Bluetongue virus exhibits membrane fusion activity. Proc. Natl. Acad. Sci. USA **101:**2100–2105.
23. **Fugier-Vivier, I., C. Servet-Delprat, P. Rivailler, M. C. Rissoan, Y. J. Liu, and C. Rabourdin-Combe.** 1997. Measles virus suppresses cell-mediated immunity by interfering with the survival and functions of dendritic and T cells. J. Exp. Med. **186:**813–823.
24. **Goder, V., and M. Spiess.** 2001. Topogenesis of membrane proteins: determinants and dynamics. FEBS Lett. **504:**87–93.
25. **Goldberg, J. L., C. L. Zanella, Y. M. Janssen, C. R. Timblin, L. A. Jimenez, P. Vacek, D. J. Taatjes, and B. T. Mossman.** 1997. Novel cell imaging techniques show induction of apoptosis and proliferation in mesothelial cells by asbestos. Am. J. Respir. Cell Mol. Biol. **17:**265–271.
26. **Gonzalez, M. E., and L. Carrasco.** 2003. Viroporins. FEBS Lett. **552:**28–34.
27. **Heinz, F. X., and S. L. Allison.** 2001. The machinery for flavivirus fusion with host cell membranes. Curr. Opin. Microbiol. **4:**450–455.
28. **Hieronymus, D. R., P. Villegas, and S. H. Kleven.** 1983. Identification and serological differentiation of several reovirus strains isolated from chickens with suspected malabsorption syndrome. Avian Dis. **27:**246–254.
29. **Higuchi, H., S. F. Bronk, A. Bateman, K. Harrington, R. G. Vile, and G. J. Gores.** 2000. Viral fusogenic membrane glycoprotein expression causes syncytia formation with bioenergetic cell death: implications for gene therapy. Cancer Res. **60:**6396–6402.
30. **Higuchi, Y.** 2003. Chromosomal DNA fragmentation in apoptosis and necrosis induced by oxidative stress. Biochem. Pharmacol. **66:**1527–1535.
31. **Huppertz, B., and J. C. Kingdom.** 2004. Apoptosis in the trophoblast—role of apoptosis in placental morphogenesis. J. Soc. Gynecol. Investig. **11:**353–362.
32. **Huppertz, B., D. S. Tews, and P. Kaufmann.** 2001. Apoptosis and syncytial fusion in human placental trophoblast and skeletal muscle. Int. Rev. Cytol. **205:**215–253.
33. **Jahn, R., T. Lang, and T. C. Sudhof.** 2003. Membrane fusion. Cell **112:**519–533.
34. **Jang, M. H., M. C. Shin, H. S. Shin, K. H. Kim, H. J. Park, E. H. Kim, and C. J. Kim.** 2002. Alcohol induces apoptosis in TM3 mouse Leydig cells via bax-dependent caspase-3 activation. Eur. J. Pharmacol. **449:**39–45.
35. **Kaneshima, H., L. Su, M. L. Bonyhadi, R. I. Connor, D. D. Ho, and J. M. McCune.** 1994. Rapid-high, syncytium-inducing isolates of human immunodeficiency virus type 1 induce cytopathicity in the human thymus of the SCID-hu mouse. J. Virol. **68:**8188–8192.
36. **Kibenge, F. S., and A. S. Dhillon.** 1987. A comparison of the pathogenicity of four avian reoviruses in chickens. Avian Dis. **31:**39–42.
37. **Kibenge, F. S. B., G. E. Gwaze, R. C. Jones, A. F. Chapman, and C. E. Savage.** 1985. Experimental reovirus infection in chickens: observations on early viraemia and virus distribution in bone marrow, liver and enteric tissues. Avian Pathol. **14:**87–98.
38. **Lama, J., and L. Carrasco.** 1995. Mutations in the hydrophobic domain of poliovirus protein 3AB abrogate its permeabilizing activity. FEBS Lett. **367:**5–11.
39. **Lamirande, E. W., D. K. Nichols, J. W. Owens, J. M. Gaskin, and E. R. Jacobson.** 1999. Isolation and experimental transmission of a reovirus pathogenic in ratsnakes (Elaphe species). Virus Res. **63:**135–141.
40. **Leland, M. M., G. B. Hubbard, H. T. Sentmore III, K. F. Soike, and J. K. Hilliard.** 2000. Outbreak of Orthoreovirus-induced meningoencephalomyelitis in baboons. Comp. Med. **50:**199–205.
41. **Lombardo, E., A. Maraver, I. Espinosa, A. Fernandez-Arias, and J. F. Rodriguez.** 2000. VP5, the nonstructural polypeptide of infectious bursal disease virus, accumulates within the host plasma membrane and induces cell lysis. Virology **277:**345–357.
42. **Loo, D. T., and J. R. Rillema.** 1998. Measurement of cell death. Methods Cell Biol. **57:**251–264.
43. **Nagata, S., H. Nagase, K. Kawane, N. Mukae, and H. Fukuyama.** 2003. Degradation of chromosomal DNA during apoptosis. Cell Death Differ. **10:**108–116.
44. **Ni, Y., and M. C. Kemp.** 1995. A comparative study of avian reovirus pathogenicity: virus spread and replication and induction of lesions. Avian Dis. **39:**554–566.
45. **O'Brien, V.** 1998. Viruses and apoptosis. J. Gen. Virol. **79:**1833–1845.
46. **Park, I. W., E. Kondo, L. Bergeron, J. Park, and J. Sodroski.** 1996. Effects of human immunodeficiency virus type 1 infection on programmed cell death in the presence or absence of Bcl-2. J. Acquir. Immune Defic. Syndr. Hum. Retrovirol. **12:**321–328.
47. **Perez, M., B. Garcia-Barreno, J. A. Melero, L. Carrasco, and R. Guinea.** 1997. Membrane permeability changes induced in Escherichia coli by the SH protein of human respiratory syncytial virus. Virology **235:**342–351.
48. **Potgens, A. J., U. Schmitz, P. Bose, A. Versmold, P. Kaufmann, and H. G. Frank.** 2002. Mechanisms of syncytial fusion: a review. Placenta **23**(Suppl. A)**:**S107–S113.
49. **Ratts, V. S., X. J. Tao, C. B. Webster, P. E. Swanson, S. D. Smith, P. Brownbill, S. Krajewski, J. C. Reed, J. L. Tilly, and D. M. Nelson.** 2000. Expression of BCL-2, BAX and BAK in the trophoblast layer of the term human placenta: a unique model of apoptosis within a syncytium. Placenta **21:**361–366.
50. **Rodrigo, A. G.** 1997. Dynamics of syncytium-inducing and non-syncytium-inducing type 1 human immunodeficiency viruses during primary infection. AIDS Res. Hum. Retrovir. **13:**1447–1451.
51. **Scheller, C., and C. Jassoy.** 2001. Syncytium formation amplifies apoptotic signals: a new view on apoptosis in HIV infection in vitro. Virology **282:**48–55.
52. **Shmulevitz, M., J. Corcoran, J. Salsman, and R. Duncan.** 2004. Cell-cell fusion induced by the avian reovirus membrane fusion protein is regulated by protein degradation. J. Virol. **78:**5996–6004.
53. **Shmulevitz, M., and R. Duncan.** 2000. A new class of fusion-associated small transmembrane (FAST) proteins encoded by the non-enveloped fusogenic reoviruses. EMBO J. **19:**902–912.
54. **Shmulevitz, M., R. F. Epand, R. M. Epand, and R. Duncan.** 2004. Structural and functional properties of an unusual internal fusion peptide in a nonenveloped virus membrane fusion protein. J. Virol. **78:**2808–2818.
55. **Skehel, J. J., and D. C. Wiley.** 2000. Receptor binding and membrane fusion in virus entry: the influenza hemagglutinin. Annu. Rev. Biochem. **69:**531–569.
56. **Solovyan, V. T., Z. A. Bezvenyuk, A. Salminen, C. A. Austin, and M. J. Courtney.** 2002. The role of topoisomerase II in the excision of DNA loop domains during apoptosis. J. Biol. Chem. **277:**21458–21467.
57. **Songserm, T., D. van Roozelaar, A. Kant, J. Pol, A. Pijpers, and A. ter**

Huurne. 2003. Enteropathogenicity of Dutch and German avian reoviruses in SPF white leghorn chickens and broilers. Vet. Res. **34**:285–295.
58. **van den Eijnde, S. M., M. J. van den Hoff, C. P. Reutelingsperger, W. L. van Heerde, M. E. Henfling, C. Vermeij-Keers, B. Schutte, M. Borgers, and F. C. Ramaekers.** 2001. Transient expression of phosphatidylserine at cell-cell contact areas is required for myotube formation. J. Cell Sci. **114:**3631–3642.
59. **van der Heide, L.** 2000. The history of avian reovirus. Avian Dis. **44:**638–641.
60. **van Niekerk, M., C. C. Smit, W. C. Fick, V. van Staden, and H. Huismans.** 2001. Membrane association of African horsesickness virus nonstructural protein NS3 determines its cytotoxicity. Virology **279:**499–508.
61. **Vieler, E., W. Baumgartner, W. Herbst, and G. Kohler.** 1994. Characterization of a reovirus isolate from a rattle snake, Crotalus viridis, with neurological dysfunction. Arch. Virol. **138:**341–344.